EXTRACTA MATHEMATICAE Vol. **12**, Núm. 1, 61 – 86 (1997)

Flaw Identification in Elastic Solids: Theory and Experiments †

A. Gesualdo, F. Guarracino, V. Mallardo
V. Minutolo and L. Nunziante

Dipartimento di Scienza delle Costruzioni, Università di Napoli "Federico II"
P. le V. Tecchio, 80-80125 *Napoli, Italy*

AMS *Subject Class.* (1991): 73–XX *Received* 18th July 1997

In this work the problem of identificating flaws or voids in elastic solids is addressed both from a theoretical and an experimental point of view. Following a so called "inverse procedure", which is based on appropriately devised experiments and a particular bounding of the strain energy, a "gap functional" for flaw identification is proposed.

1. Direct and Inverse Problems

The modern theory of elasticity and its related methods of solution by discretization techniques are nowadays able to solve practically any structural problem which is formulated in the direct way.

Let us make reference to the linearly elastic equilibrium problem represented by the well-known Navier-Cauchy field equations (see fig. 1)

$$\mu\triangle^2\mathbf{u}(\mathbf{x}) + (\lambda+\mu)\nabla\,\mathrm{div}\,\mathbf{u}(\mathbf{x}) + \mathbf{b}(\mathbf{x}) = \mathbf{0}\ , \quad \mathbf{x}\in\dot{V} \tag{1}$$

with associated Neumann's conditions on the free boundary

$$(\mathbf{C}\,\mathrm{Sym}\,\nabla\mathbf{u})\mathbf{n} = \mathbf{t}\ , \quad \mathbf{x}\in\partial V_{\mathbf{t}} \tag{2}$$

and Dirichlet's ones on the constrained boundary

$$\mathbf{u} = \mathbf{u}_0\ , \quad \mathbf{x}\in\partial V_{\mathbf{u}} \tag{3}$$

†Editor's Note: This paper was presented in the "Third Metting on Current Ideas in Mechanics and Related Fields" celebrated in Segovia (Spain) in June 1995 and it was intended to appear in Extracta Mathematicae, Vol. 11, Núm. 1 (1996), where all the contributions to this metting were collected.

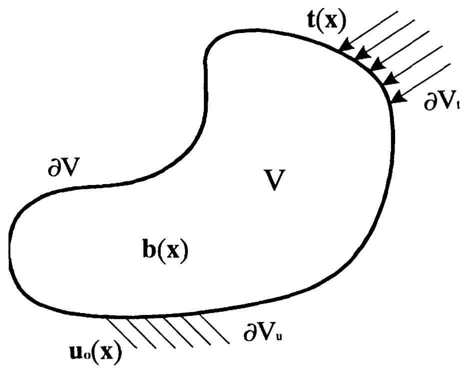

Figure 1.

In the above equation $\mathbf{u}(\mathbf{x})$ is the unknown displacement field defined on the domain $V \subseteq E^3$ occupied by the solid, λ and μ are the Lamé's elastic constants for an homogeneous and isotropic material, $\mathbf{b}$ is the volume forces field, $\mathrm{Sym}\,\nabla\mathbf{u}$ is the infinitesimal deformation tensor, $\mathbf{C}$ is the symmetric tensor of the elastic constants (depending on λ and μ). Moreover, $\mathbf{T} = \mathbf{C}\,\mathrm{Sym}\,\nabla\mathbf{u}$ is the Cauchy stress tensor, $\mathbf{n}$ is the outward unit normal field on ∂V, $\mathbf{t}$ is the traction field on $\partial V_{\mathbf{t}}$ and $\mathbf{u}_0$ is the displacement field imposed on the costrained boundary $\partial V_{\mathbf{u}}$.

As *direct formulation* we mean that formulation of the problem of the elastic equilibrium in which the geometry, the elastic constants and the field equations, together with the boundary conditions, are assigned, while displacements, strains, stresses and tractions result unknown.

Known quantities:

$$V,\ \partial V_{\mathbf{t}},\ \partial V_{\mathbf{u}},\ \lambda,\ \mu,\ \mathbf{C},\ \mathbf{b},\ \mathbf{t}(\mathbf{x})\ \ \forall\mathbf{x}\in\partial V_{\mathbf{t}},\quad \mathbf{u}_0(\mathbf{x})\ \ \forall\mathbf{x}\in\partial V_{\mathbf{u}}\,.$$

Unknown quantities:

$$\mathbf{u}(\mathbf{x}),\ \varepsilon = \mathrm{Sym}\,\nabla\mathbf{u},\ \sigma = \mathbf{C}\,\mathrm{Sym}\,\nabla\mathbf{u},\ \sigma\mathbf{n} = \mathbf{t} \qquad \forall\mathbf{x}\in\partial V_{\mathbf{u}}\,.$$

Recently, in the material and structural engineering the problem of the elastic equilibrium in the so called *inverse formulation* is becoming more and more important. In fact, this formulation allows to deal with relevant questions of civil, aeronautic and mechanical engineering.

As a matter of fact the actual behaviour of real systems can be quite different from the theoretical one.

With reference to the equilibrium of linearly elastic solids, it may happen that:

- the bonds assigned on the boundary may be governed by equations which are quite different from the modelled ones, this on account of local effects arisen during the construction (as building imperfections, yieldings or distorsions);
- inhomogeneities and anisotropies may take place in some zones, voids and inclusions of different materials may be present and modify the structural response;
- flaws, delaminations or detachments may be present in the volume or in proximity of the boundary. These defects may arise during the loading history, or be present in the construction from the beginning.

Therefore, as *inverse formulation* we mean that formulation of the problem of the elastic equilibrium in which the field equations are assigned, and the displacement field is known, having been experimentally read on the boundary. On the contrary, some data which are given in the direct formulation in this case result unknown and need to be identified. In particular the unknown quantities may be:

- the effective geometry of the solid and of the nonvisible boundaries, if any;
- the elastic constants of the material and the density of some parts of the solid;
- the body forces and/or the boundary tractions;
- displacement, strain and stress fields inside the region occupied by the body.

A table of possible perturbations which can take place in actual cases is given in the fig. 2.

In such cases the inverse problem presents further unknown entities:

- an internal boundary ∂V_i of a void ω;
- an internal surface S due to a detachment;
- an inclusion $V_{\mu'}$ of material with different elastic costants;
- a sub-domain $V_{b'}$ with different density.

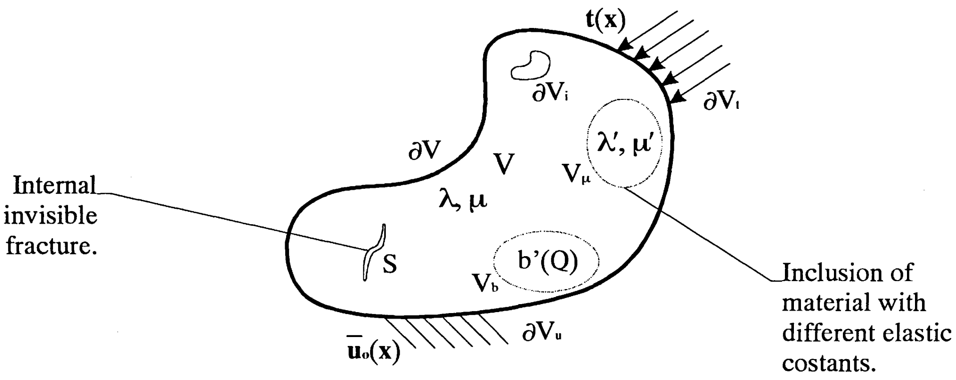

Figure 2.

It is obvious that the above mentioned problem may not result generally solvable. With reference to the single perturbation, however, it is possible to identify its effects on the structural behaviour and, consequently, its entity and position. This happens by means of laboratory and numerical experiments, which can provide a full set of data on the boundary of the real solid and allow a comparison with the theoretical behaviour of the "perfect solid".

Object of this paper is the study of the presence of invisible voids or detachments at the inside of the solid and the development of some theoretical tools apt to identify these flaws, that is a specially designed "gap functional".

The background of this work lies on some simple concepts of fracture mechanics, as well as on the recent development of inverse methods [Mura, 1982; Natke, 1994; Bui, 1993]. It is worth noticing that some of the following theoretical result have already been deducted [Villaggio, (1977)] by means of a complementary energy approach.

2. The Elastic Solid with a Small Flaw

In this section we tackle two problems in the field of linear elastostatics.

The first one is represented by the presence of a small flaw inside a linearly elastic solid, i.e. a detachment on an internal surface S on account of the occurrence of a very small discontinuity between two faces. This surface S may join the boundary of the solid or not. Without respect to the way in which the detachment took place, in this paper it is proved that under prescribed loads and fixed constraints the solid embeds an elastic energy W^D which is greater than the energy embedded in the same solid in absence of the flaw and under the same loading. The bounding of the strain energy leads to a bounding of the generalised displacements of the loaded parts of the boundary as well.

The second problem is represented by the above introduced solid in which also an anelastic strain field is present. This stands for the very actual case of solids in which fractures, delaminations or other defects are joined by inelastic deformations and by a system of relevant self stresses [Lippman, 1977].

The proved theorems, however simple, seem promising of interesting results in the identification of internal defects by coupling numerical analysis and experimental data, as it has been already widely shown [Bui and Tanaka, 1994; Rice, 1968; Popelar and Kanninen, 1985; Bittanti, Maier and Nappi, 1984; Mroz, 1994; Guarracino et al., 1995; Nunziante et. al., '95].

2.1. The Case of Applied Tractions. Let us start our discourse by considering an homogeneous linearly elastic solid V_1 (fig. 3.a), with mixed boundary conditions. This *first problem* will be called "the problem of the integer solid".

The case of fixed constraints and applied loads is now treated: the same line of reasoning leads to similar results in the case of zero tractions and prescribed boundary displacements.

Let $\mathbf{u}^1$ be the unique displacement field solution of the Navier-Cauchy equations for the "integer solid", and ε^1 the strain tensor field derived by $\mathbf{u}^1$ as the symmetric part of the gradient of $\mathbf{u}^1$. The stress tensor σ^1 can be obtained by ε^1 by the well known stress-strain relationship $\sigma^1 = \mathbf{C}\,\varepsilon^1$.

Let us then consider a *second problem* consisting of a solid V (fig. 3.b) featuring the same shape, the same material constants, fixed constraints and applied loads of the first one. The only difference lies in the presence of a flaw at the internal surface S. We operate in the framework of the infinitesimal displacement theory of elasticity, and suppose that the flaw is an infinitesimal detachment of the two sides of the surface S, without any loss of material. Under this assumption the volume ω included in the surface S may be considered as vanishing. In correspondence with S a jump of the displacement field may take place. The surface S is assumed to be regular almost everywhere.

Let $\mathbf{n}$ be the unit outward normal vector field at the regular points of S, $\mathbf{u}$ the unique displacement field solution of the second problem and ε and σ the strain and stress fields, respectively. For the moment let us suppose that in the detached solid there are no self stresses, as it may happen on account of inelastic effects yielded by the detachment.

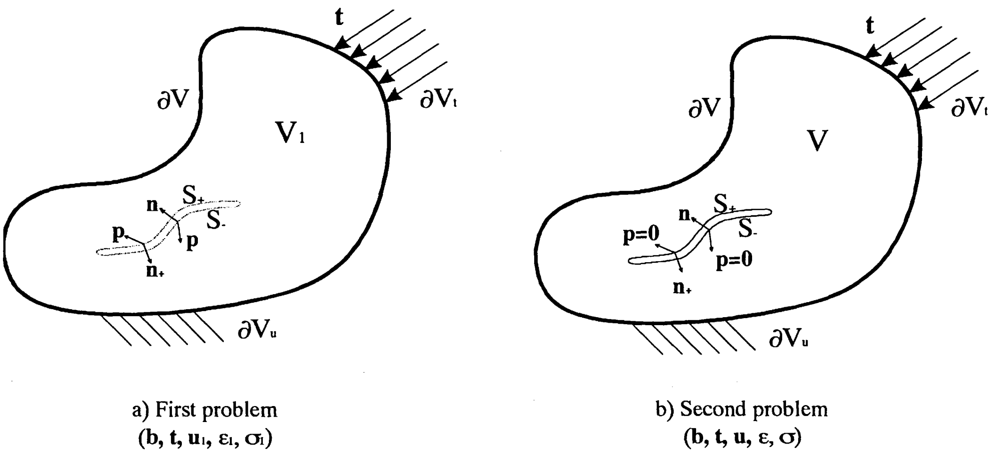

Figure 3.

Moreover, let $\mathbf{p}$ be the traction vector field acting on the surface S of normal $\mathbf{n}$ in the integer solid, and whose value is yielded by the equation:

$$\mathbf{p} = \sigma^1 \, \mathbf{n} \tag{4}$$

$\mathbf{p}$ is supposed to be non zero everywhere.

Now we wish to compare the integer solid with the detached one.

Thanks to the infinitesimal displacement assumption, the displacement field $\mathbf{u}$ in V of the detached solid can be regarded as the sum of the solution of the integer one and of the solution $\overline{\mathbf{u}}$ of a *third problem* (see fig. 4) which consists of the detached solid loaded on S by the opposite of the already computed surface tractions (4), i.e. $-\mathbf{p} = -\sigma^1 \, \mathbf{n}$.

Therefore the following relationships hold true:

$$\mathbf{u} = \mathbf{u}^1 + \overline{\mathbf{u}}\,, \quad \varepsilon = \varepsilon^1 + \overline{\varepsilon}\,, \quad \sigma = \sigma^1 + \overline{\sigma}\,. \tag{5}$$

Application of Clapeyron's theorem to the third, the first and the second problem, respectively, leads to:

$$-\int_S \mathbf{p} \; \overline{\mathbf{u}} \; dS = \int_V \overline{\sigma} \; \overline{\varepsilon} \; dV = 2 \; \overline{W} > 0 \tag{6}$$

$$\int_{\partial V} \mathbf{t} \; \mathbf{u}^1 dS + \int_V \mathbf{b} \; \mathbf{u}^1 \; dV = \int_V \sigma^1 \varepsilon^1 dV = 2 \; W \tag{7}$$

$$\int_{\partial V} \mathbf{t}\ \mathbf{u}\ dS + \int_V \mathbf{b}\ \mathbf{u}\ dV = \int_V \sigma\ \varepsilon\ dV = 2\ W^D \tag{8}$$

where, $\overline{W}$, W and W^D are the elastic strain energy of the third problem, of the "integer solid" and of the "detached solid", respectively.

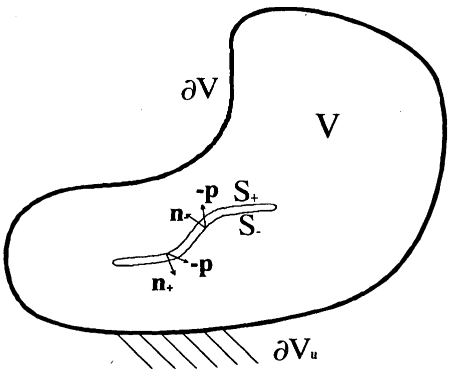

Figure 4: Third problem $(-\mathbf{p}, \bar{\mathbf{u}}, \bar{\varepsilon}, \bar{\sigma})$.

As the volume ω of the flaw is infinitesimal, the domains of the two problems coincide.

By virtue of the equations (6), (7) and (8), and by taking into account that

$$\int_V \overline{\sigma}\ \varepsilon^1 dV = 0 = -\int_S \mathbf{p}\ \mathbf{u}^1 dS$$

as the stress field $\overline{\sigma}$ corresponds to the self-equilibrated traction field $-\mathbf{p}$ on S and $\mathbf{u}^1$ is continuous on S, we have

$$\begin{aligned} 2\ W^D &= \int_V \sigma\ \varepsilon\ dV = \int_V (\sigma^1 + \overline{\sigma})(\varepsilon^1 + \overline{\varepsilon})\ dV \\ &= \int_V \sigma^1 \varepsilon^1 dV + \int_V \overline{\sigma}\ \overline{\varepsilon}\ dV + 2 \int_V \overline{\sigma}\ \varepsilon^1 dV = 2\ W + 2\ \overline{W}. \end{aligned}$$

Hence the following inequality holds true

$$W^D > W \tag{9}$$

and proves that:

THEOREM 1. *The elastic solid with a small internal flaw and subject to any applied loads and fixed constraints, presents a strain energy* W^D *which is greater than the energy* W *accumulated by the integer one under the same loads and constraints.*

When a generalised force-displacement theory can be established, as it is the case of rods, beams, plates and shells, inequality (9) gives

$$(\mathbf{F}\ \mathbf{u}) > (\mathbf{F}\ \mathbf{u}^1) \tag{10}$$

provided there are null volume forces ($\mathbf{b} = \mathbf{0}$), and the tractions consist of a single point load $\mathbf{F}$. This is equivalent to

$$u_F > u_F^1 \tag{11}$$

where u_F and u_F^1 are the generalised components of displacement of the loaded points in the direction of $\mathbf{F}$, with reference to the detached solid and to the integer one, respectively. The following theorem is thus proved:

THEOREM 2. *Let us consider a structural framework for which a generalised force-displacement theory exists. Let an integer solid be subject to fixed constraints and to the action of a single generalised force* $\mathbf{F}$, *and let us take into consideration a second solid with a small internal flaw which is subject to the same loading and constraint conditions of the previous one. Under these assumptions the generalised displacement* u_F *in the direction of the force* $\mathbf{F}$ *of the loaded point of the detached solid results greater than the corresponding value* u_F^1 *of the same point of the integral one.*

It is noteworthy that, having determined by means of simple experiment the displacement u_F , the comparison with the theoretical value u_F^1 of the integer solid leads to a necessary condition for the existence of an internal detachment in the solid under analysis.

2.2. THE CASE OF APPLIED DISPLACEMENTS. In the case of zero applied tractions and non zero prescribed displacements of a part ∂V_u of the boundary, a procedure similar to that of the previous number leads to corresponding results. In fact, with reference to fig. 5, let us consider the problem 5.a of an integer solid subject to prescribed displacements $\mathbf{u}^*$ on the constrained part ∂V_u of the boundary and to zero tractions $\mathbf{t} = \mathbf{0}$ on the free boundary ∂V_t. The volume forces are zero as well, i.e. $\mathbf{b} = \mathbf{0}$. Let $\mathbf{u}^i$, ε^i, σ^i be the solution of this problem, and W^i the corresponding strain energy.

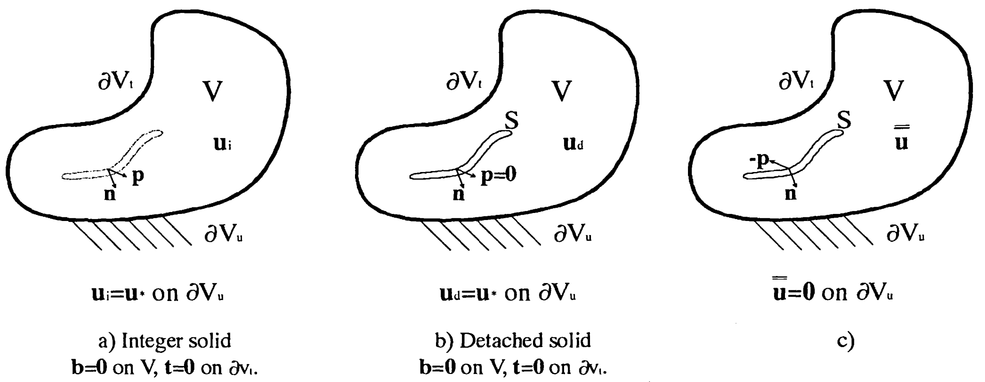

Figure 5.

Let us then consider the problem 5.b represented by the same solid with an internal detachment in correspondence with the internal surface S and subject to the same boundary conditions. Be $\mathbf{u}^d$, ε^d, σ^d the fields solution of this case. Finally, let us take into account the detached solid of fig. 5.c with fixed constraints $\mathbf{u} = \mathbf{0}$ on ∂V_u, and loaded on the surface S by the tractions $-\mathbf{p} = -\sigma^i \mathbf{n}$ which correspond to the ones evaluated for the integer solid. Be $\overline{\overline{\mathbf{u}}}$, $\overline{\overline{\varepsilon}}$, $\overline{\overline{\sigma}}$ the solution of this problem.

In this case the following relationships hold true:

$$\mathbf{u}^d = \mathbf{u}^i + \overline{\overline{\mathbf{u}}}\,, \quad \varepsilon^d = \varepsilon^i + \overline{\overline{\varepsilon}}\,, \quad \sigma^d = \sigma^i + \overline{\overline{\sigma}}$$

and it follows

$$\begin{aligned} 2\ W^i &= \int_V \sigma^i \varepsilon^i dV = \int_V \left(\sigma^d - \overline{\overline{\sigma}}\right)\left(\varepsilon^d - \overline{\overline{\varepsilon}}\right)\ dV \\ &= \int_V \sigma^d \varepsilon^d dV + \int_V \overline{\overline{\sigma}}\,\overline{\overline{\varepsilon}}\ dV - 2\int_V \sigma^d\,\overline{\overline{\varepsilon}}\ dV = 2\ W^d + 2\ \overline{\overline{W}} \end{aligned}$$

where W^i, W^d and $\overline{\overline{W}}$ represent the strain energy of the previous problems, respectively. In fact we have:

$$\int_V \sigma^d\,\overline{\overline{\varepsilon}}\ dV = \int_{\partial V \cup S} \mathbf{t}^d\,\overline{\overline{\mathbf{u}}}\ dS = 0\,.$$

As $\mathbf{t}^d = \mathbf{0}$ on ∂V_t, $\overline{\overline{\mathbf{u}}} = \mathbf{0}$ on ∂V_u and $\mathbf{p} = \mathbf{0}$ on S. Therefore it is

$$W^i > W^d\,, \tag{12}$$

i.e. an inequality correspondent to the above proved (9).

Hence the following theorem holds true:

THEOREM 3. *Let us consider an elastic solid with an internal flaw and subject to prescribed and not identically vanishing displacements* $\mathbf{u}^*$ *on the constrained part of the boundary, to zero applied tractions on* ∂V_t *and to zero volume forces in* V. *The comparison between this solid and the corresponding "integer solid" (in which the detachment is not present) subject to the same displacement field* $\mathbf{u}^*$ *of the constraints, shows that the strain energy* W^d *of the first is smaller than that* W^i *of the integer solid.*

2.3. THE PRESENCE OF DISTORTIONS AND SELF STRESSES IN THE DETACHED SOLID. Let a strain field be initially present in the above considered detached solid (number 2.1). We suppose that it can be represented as $\varepsilon^* = \varepsilon_p^* + \varepsilon_e^*$, i.e. by means of the sum of a distortional and kinematically not compatible part ε_p^*, and of an elastic part ε_e^* which makes compatible the resulting field ε^* . In order to avoid the trivial case, let us suppose that $\varepsilon_e^* \neq \mathbf{0}$ almost everywhere.

In this solid a system of self stresses takes place. Its value is given by the constitutive relationships:

$$\sigma^* = \mathbf{C}\,\varepsilon_e^* . \tag{13}$$

The displacements $\mathbf{u}^s$, the strains ε^s and the stresses σ^s, which constitute the solution of this problem ("*fourth problem*") are represented by the following equations, in virtue of the superposition principle:

$$\begin{aligned}
\mathbf{u}^s &= \mathbf{u} + \mathbf{u}^* = \mathbf{u}^1 + \overline{\mathbf{u}} + \mathbf{u}^* ,\\
\varepsilon^s &= \varepsilon + \varepsilon^* = \varepsilon^1 + \overline{\varepsilon} + \varepsilon^* = \varepsilon^1 + \overline{\varepsilon} + \varepsilon_e^* + \varepsilon_p^* ,\\
\sigma^s &= \sigma + \sigma^* = \sigma^1 + \overline{\sigma} + \sigma^* .
\end{aligned}$$

The starred elements correspond to the presence of the distortion, while the quantities denoted by the bar or the superscript 1, retain the same meaning as before (see figs. 3.a, 3.b and 4).

Now we want to evaluate the effect of the distortions on the strain energy of the detached solid. In particular we want to compare the elastic strain energy $W^P$of this fourth problem, in which self stresses are present, with the value W^D attained in the same solid in absence of self stresses (second problem in the number 2.1).

The strain energy of the detached solid is given by:

$$W^D = \frac{1}{2}\int_V \left(\sigma^1 + \overline{\sigma}\right)\left(\varepsilon^1 + \overline{\varepsilon}\right)\, dV = \frac{1}{2}\int_V \left(\varepsilon^1 + \overline{\varepsilon}\right)\, \mathbf{C}\, \left(\varepsilon^1 + \overline{\varepsilon}\right)\, dV \tag{14}$$

while the strain energy of the fourth problem has the following value

$$W^P = \frac{1}{2}\int_V \left(\varepsilon^1 + \overline{\varepsilon} + \varepsilon^*_e\right)\, \mathbf{C}\, \left(\varepsilon^1 + \overline{\varepsilon} + \varepsilon^*_e\right)\, dV\,. \tag{15}$$

Therefore it follows

$$W^P - W^D = \frac{1}{2}\int_V \varepsilon^*_e\, \mathbf{C}\, \varepsilon^*_e\, dV + \int_V \left(\sigma^1 + \overline{\sigma}\right)\, \varepsilon^*_e\, dV\,. \tag{16}$$

By virtue of the positive definiteness of the first integral at the right hand term, the previous equation shows that, provided

$$\int_V \left(\sigma^1 + \overline{\sigma}\right)\, \varepsilon^*_e\, dV > 0 \tag{17}$$

holds true, we have

$$W^P > W^D\,. \tag{18}$$

Hence the strain energy of the detached solid with self stresses is greater than that of the solid without self stresses.

Coupling equation (9) and (18), we obtain the inequality chain

$$W^P > W^D > W \tag{19}$$

and we prove the following theorem:

THEOREM 4. *The presence of an inelastic strain field with related self stresses in a solid which features a small internal flaw and is subject to surface and volume forces and to fixed constraints, leads to an elastic strain energy W^P greater than the one W^D corresponding to the absence of such self stresses. This happens provided eq.(17) holds true.*

On the contrary, if the following inequality holds true:

$$\int_V \left(\sigma^1 + \overline{\sigma}\right)\, \varepsilon^*_e\, dV < -\frac{1}{2}\int_V \varepsilon^*_e\, \mathbf{C}\, \varepsilon^*_e\, dV\,, \tag{20}$$

then we have

$$W^P < W^D \tag{21}$$

and the strain energy of the detached solid results greater than the one of the solid in which the self-stresses are present.

3. Effects Due to the Presence of a Void in an Elastic Solid

It often happens that during the manufacturing process, some undesirable voids may take place in structural elements. It is therefore necessary to develop suitable procedures in order to allow the detection of the cavity.

Thus, let us address the problem of a solid V featuring an internal void ω with an unknown boundary S. We will reason under the same hypotheses of the previous section, namely homogeneous linearly elastic material, infinitesimal displacements and a suitable degree of smoothness of the boundaries ∂V and S. For the sake of clarity, we consider only tractions $\mathbf{t}$ and volume forces $\mathbf{b}$, together with fixed constraints di ∂V_u. We want to compare the solution of this elastic equilibrium problem, which we call "problem 2", with that of the same solid without the void ω of volume V_1, which we call "problem 1" (see fig. 6).

Problem 1 ($\mathbf{b}$, $\mathbf{t}$, $\mathbf{u}_1$, ε_1, σ_1) Problem 2 ($\mathbf{b}$, $\mathbf{t}$, $\mathbf{u}$, ε, σ)

Figure 6.

The volume forces will obviously vanish only in the region ω of problem 2.

Let ($\mathbf{b}$, $\mathbf{t}$, $\mathbf{u}_1$, ε_1, σ_1) and ($\mathbf{b}$, $\mathbf{t}$, $\mathbf{u}$, ε, σ) be the sets of loads, displacements, strain and stress fields of problems 1 and 2, respectively.

The solution of problem 2 will evidently present zero tractions on S.

We want to establish a relationship between the strain energy of problem 1 and that of problem 2. The volume of solid 1 is V and that of solid 2 is V_1, being $\mathrm{V}=\mathrm{V}_1 \cup \omega$.

Application of Clapeyron's theorem to problems 1 and 2, allows us to write

$$\int_{\partial V} \mathbf{t}\ \mathbf{u}_1 dS + \int_{V_1} \mathbf{b}\ \mathbf{u}_1 dV + \int_{\omega} \mathbf{b}\ \mathbf{u}_1 dV = \int_{V_1} \sigma_1 \varepsilon_1 dV + \int_{\omega} \sigma_1 \varepsilon_1 dV = 2\ W \tag{22}$$

$$\int_{\partial V} \mathbf{t}\ \mathbf{u}\ dS + \int_{V_1} \mathbf{b}\ \mathbf{u}\ dV = \int_{V_1} \sigma\ \varepsilon\ dV = 2\ W_V \tag{23}$$

where W and W_V are the strain energies of the solid in absence and in presence of the void, respectively.

In what follows we apply the Virtual Work Equation (VWE) to particular equilibrated forces-stresses fields and compatible displacement-strains fields; the VWE will be applied to the intersection of the domains V and V_1, i.e. V_1=V∩V_1.

The solution of problem 2 ($\mathbf{b}$, $\mathbf{t}$, $\mathbf{u}$, ε, σ) can be obtained by superposition of two systems (see fig. 7): the first is the restriction of the solution of problem 1 to the volume V_1, the second is the solution corresponding to the application of the stresses $-\mathbf{p}$ on the internal surface S (they represent the action of ω on V_1).

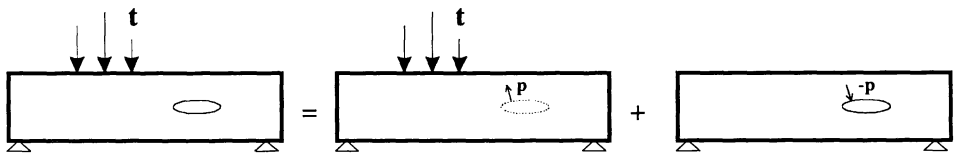

Figure 7.

We have:

$$\mathbf{u} = \mathbf{u}_1 + \overline{\mathbf{u}}\,, \quad \varepsilon = \varepsilon_1 + \overline{\varepsilon}\,, \quad \sigma = \sigma_1 + \overline{\sigma} \qquad \mathbf{x} \in V_1 \tag{24}$$

We can insert these relationships in the (23) and perform a comparison with (22), obtaining

$$-\int_\omega \mathbf{b}\ \mathbf{u}_1 dV + \int_\omega \sigma_1\varepsilon_1 dV + \int_{\partial V} \mathbf{t}\ \overline{\mathbf{u}}\, dS + \int_{V_1} \mathbf{b}\ \overline{\mathbf{u}}\ dV$$
$$= 2\int_{V_1} \sigma_1\overline{\varepsilon}\, dV + \int_{V_1} \overline{\sigma}\,\overline{\varepsilon}\, dV\,. \tag{25}$$

By means of the application of the VWE to particular states of equilibrated forces-stresses and compatible displacement strains, we have

VWE 1-2" $$\int_{\partial V} \mathbf{t}\overline{\mathbf{u}} dS + \int_{V_1} \mathbf{b}\overline{\mathbf{u}} dV + \int_S \mathbf{p}\overline{\mathbf{u}} dS = \int_{V_1} \sigma_1\overline{\varepsilon} dV \tag{26}$$

VWE 2"-2" $$-\int_S \mathbf{p}\overline{\mathbf{u}} dS = \int_{V_1} \overline{\sigma}\overline{\varepsilon} dV \tag{27}$$

We can now combine (26) and (27)

$$\int_{\partial V} \mathbf{t}\,\overline{\mathbf{u}}\,dS + \int_{V_1} \mathbf{b}\,\overline{\mathbf{u}}\,dV = \int_{V_1} \bar{\sigma}\,\bar{\varepsilon}\,dV + \int_{V_1} \sigma_1 \bar{\varepsilon}\,dV \tag{28}$$

and insert the result in (25), getting

$$\int_{V_1} \sigma_1\,\bar{\varepsilon}\,dV = -\int_{\omega} \mathbf{b}\,\mathbf{u}_1\,dV + \int_{\omega} \sigma_1 \varepsilon_1 dV\,. \tag{29}$$

By substituting (29) in (28), as we have

$$\int_{V_1} \bar{\sigma}\,\bar{\varepsilon}\,dV > 0\,, \quad \int_{\omega} \sigma_1 \varepsilon_1\,dV > 0\,, \quad \overline{\mathbf{u}} = \mathbf{u} - \mathbf{u}_1\,,$$

we get

$$\int_{\partial V} \mathbf{t}\,\mathbf{u}\,dS + \int_{V_1} \mathbf{b}\,\mathbf{u}\,dV - \int_{\partial V} \mathbf{t}\,\mathbf{u}_1\,dS - \int_{V_1} \mathbf{b}\,\mathbf{u}_1\,dV + \int_{\omega} \mathbf{b}\,\mathbf{u}_1\,dV = 0\,. \tag{30}$$

Finally we can rearrange this equation to obtain

$$W_V > W - \int_{\omega} \mathbf{b}\,\mathbf{u}_1\,dV\,. \tag{31}$$

Hence, the strain energy W_V of an homogeneous and linearly elastic solid, which is subject to fixed constraints and prescribed loads ($\mathbf{t}$, $\mathbf{b}$) and features an internal void, satisfies the inequality (31). W is the strain energy of the same problem in absence of voids. Equation (31) makes possible to deduce a full class of useful inequalities with reference to the displacements of loaded points, as we have already done in Sect. 2.1.

4. A Gap Functional for the Identification of Internal Flaws

In this section a "gap functional" for the identification of internal flaws and relevant displacement discontinuities in a linearly elastic body is proposed.

This functional is based on the sole knowledge of the boundary displacement field and can lead to the identification of both position and shape of the internal discontinuity. The case of zero volume forces will be treated.

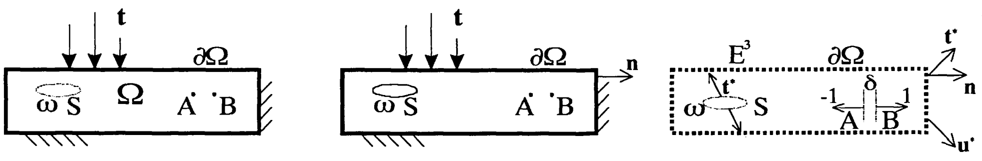

a) Elastic body Ω, displacement field $\bar{\mathbf{u}}$.

b) Elastic body Ω with a flow ω in S; displacement field **u**.

c) Three-dimensional elastic space E^3; displacement solution due to a dipole of unitary forces $\mathbf{u}^*$; relevant tractions $\mathbf{t}^*$.

Figure 8.

Let $\bar{\mathbf{u}}$ be the boundary displacement field of the integer solid Ω. It can be obtained by means of experimental or numerical tests, following the application of tractions $\mathbf{t}$ on the free boundary $\partial\Omega_t$. $\bar{\mathbf{r}}$ is the reaction field (fig. 8a) on the constrained boundary $\partial\Omega_u$.

Let $\mathbf{u}$ be the boundary displacement field of the same elastic solid Ω featuring an internal void ω which is surronded by the boundary S. The boundary displacement field and the reaction field $\mathbf{r}$ may be obtained by means of a suitable experimental technique.

Let us finally consider an auxiliary problem constituted by the three-dimensional elastic space E^3 which is loaded by a pair of opposite unit forces acting in the x_i direction and applied at the points A and B, whose distance is δ. The solution $\mathbf{u}^*$ of this problem is obtained by superposing the Kelvin's fundamental solutions (fig. 8c) corresponding to each unit load. The traction field on the surface corresponding to the boundary of the solid Ω is denoted as $\mathbf{t}^*$.

The solutions $\bar{\mathbf{u}}$ and $\mathbf{u}^*$ are restricted to the domain of the fractured solid $\Omega - \omega$.

The fact that on the boundary $\partial\Omega$ the difference $\mathbf{v} = \bar{\mathbf{u}} - \mathbf{u}$ does not vanish everywhere, constitutes a condition which is sufficient to reveal the presence of the expected defect:

$$\mathbf{v} = \bar{\mathbf{u}} - \mathbf{u} \neq 0 , \qquad \mathbf{x} \in \partial\Omega . \tag{32}$$

The displacement field $\mathbf{v}$ corresponds to vanishing boundary tractions $\delta\mathbf{t}$ on $\partial\Omega_t$ and to the reactions

$$\delta\mathbf{r} = \bar{\mathbf{r}} - \mathbf{r} . \tag{33}$$

The application of the reciprocity equation to the elastic states $\mathbf{u}^*$ and $\mathbf{v}$ leads to the following integral equation, which is referred to the domain $\Omega - \omega$

$$1 \cdot \Delta v_i^{AB} + \int_{\partial\Omega} \mathbf{t}^* \mathbf{v} \; dS + \int_S \mathbf{t}^* \mathbf{v} \; dS = \int_{\partial\Omega_t} \delta \mathbf{t} \; \mathbf{u}^* dS + \int_{\partial\Omega_u} \delta \mathbf{r} \; \mathbf{u}^* dS \,. \quad (34)$$

As known, this is an integral relationship of the Somigliana's type.

If we take into account the fact that $\partial \mathbf{t} = 0$ as the problems (a) and (b) are subject to the same tractions, it turns out that equation (34) can be read as

$$1 \cdot \Delta v_i^{AB} + \int_S \mathbf{t}^* \mathbf{v} \; dS = - \int_{\partial\Omega} \mathbf{t}^* \mathbf{v} \; dS + \int_{\partial\Omega_u} \delta \mathbf{r} \; \mathbf{u}^* dS \,. \quad (35)$$

It is worth noticing that the left hand term of equation (35) cannot be evaluated directly because it involves unknown quantities. It defines the so called "differential gap functional"

$$G = \Delta v_i^{AB} + \int_S \mathbf{t}^* \mathbf{v} \; dS \quad (36)$$

whose values can be calculated by means of the right hand term of equation (35). This involves only known boundary quantities, and requires a suitable numerical procedure dealing with experimental data.

A simple analysis leads to the following results:

(1) $G = 0$ is a necessary condition for $\mathbf{v} = 0$ and $\mathbf{u} = \overline{\mathbf{u}}$ and, consequently, to state the absence of voids.

(2) $G \neq 0$ is a sufficient condition for a void to be present.

In this case it is possible to decompose G in the form

$$G = \Delta v_i^e + \Delta v_i^J + \int_S \mathbf{t}^* \mathbf{v} \; dS \quad (37)$$

where:

Δv_i^e is the elastic part of the displacement difference;

Δv_i^J is the jump in the displacement field; this value is obviously zero if the pair of unit forces does not lie across a fracture, on the contrary it results non zero if the line between the collocation points A and B passes through a fracture.

The term $\int_S \mathbf{t}^* \mathbf{v} \; dS$ can be noticeable when a fracture is present and the force doublet is collocated nearby. As a result the sum $(\Delta v_i^J + \int_S \mathbf{t}^* \mathbf{v} \; dS)$

tends to an extremum value when the collocation points A and B lay across the unknown fracture.

The numerical evaluation of the functional G for a discrete and suitable choice of collocation points will allow the identification of the position and shape of any flaw.

It is noteworthy that the experimental mapping of the boundary fields requires a suitable technique which in any case must be related to the extent of the unknown flaw.

5. An Identification Procedure Based on Laser Holographic Techniques

The theoretic development presented in the previous sections has been successfully applied to the identification of flaws in Plexiglas specimens in conjunction with an experimental technique based on laser holography.

The goal of the proposed identification procedure consists in deriving information about the internal structure of the body and in particular about the position and size of possible flaws.

In order to accomplish this, from the previous discourse it stems that it is necessary to follow two steps:

- acquisition of boundary data;
- formulation of a theoretical procedure and of a relevant numerical algorithm aimed to the identification of defects.

With reference to the first step, there are two major requirements:

(a) a high accuracy even for a very low level of applied loads;

(b) a fine meshing of the boundary data.

For both the above reasons it seemed appropriate to employ a laser holographic interferometer for the experimental mapping of boundary displacement fields.

With reference to the second step, there are three major requirements:

(a) a low amount of computation;

(b) an high accuracy of the numerical results;

(c) making reference to the sole boundary values.

The natural choice is therefore a boundary integral approach.

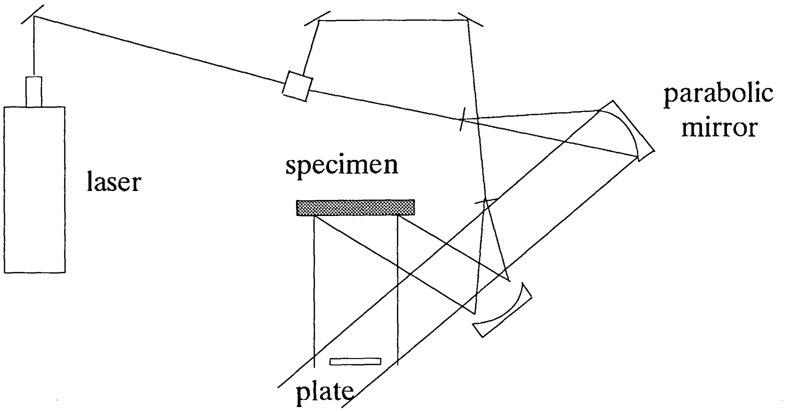

Figure 9-a.

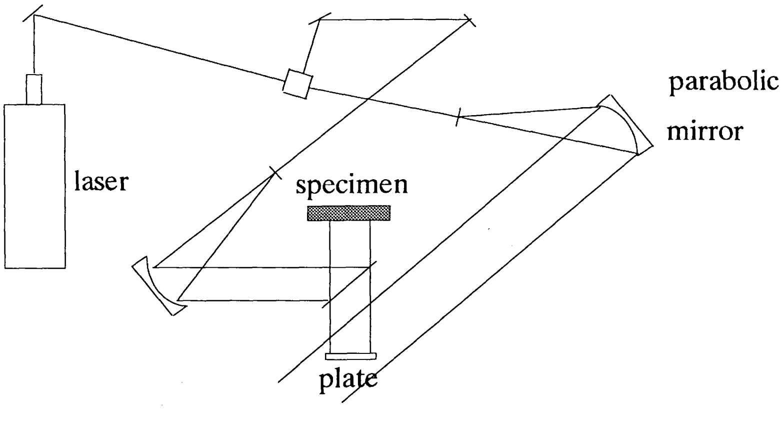

Figure 9-b.

5.1. ACQUISITION OF EXPERIMENTAL DATA. Figures 9.a and 9.b refer to the holographic desk used. It consists of a laser source, two parabolic mirrors, and a computer to process the data. A holographic interferometery technique with double exposition was employed.

The laser beam is split into two different rays. The first one (reference ray) goes directly to the film (AGFA holographic film BE75), while the second one is directed to the specimen under analysis.

Both rays are expanded by means of a microscopic lens and filtered by means of a pin-hole. They successively reach two parabolic mirrors which in turn determine two plane wave fronts.

As result a picture representing the displacement field in the form of diffraction lines is obtained. The value of the wave length is 0.632μm, and this determines the level of precision achievable.

Three specimens were tested. They were all 180mm long, 30mm high and 9.7mm wide, but the first had no flaws, the second an horizontal crack and the third a vertical one. Both the horizontal and the vertical cracks measured 10mm, with the centre at 65mm from the left external side (fig. 10).

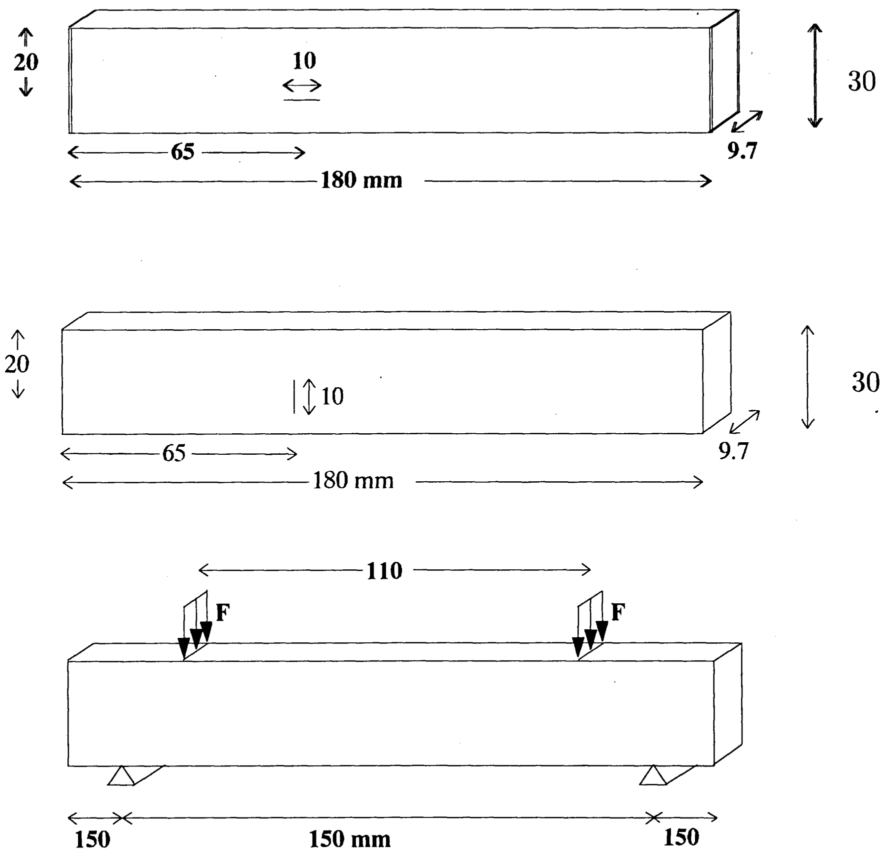

Figure 10.

The three samples were simply supported at A and B and were loaded by two concentrated forces in the range of $1.5 \div 3$kg. They were symmetrically placed at 55mm from the centres of the specimens. The supports were symmetrically placed at 75mm from the centre (fig. 10).

With the holographic result for the specimen without flaws, it has been possible to evaluate the displacement field on the inferior and lateral sides of the specimen making reference to the number and the shape of the dark lines. There was a lack of symmetry due to the non-perfectly symmetrical application of the loads, which gave origin to a torsional deformation mode in addition to the expected bending one.

The holographic result for the vertical flaw showed dark lines which were more dense on the flawed side, which denotes increased displacement values.

Fig. 11 shows the displacement diagram for an horizontal line at the bottom face of the three specimens. The maximum values are in the range of 18.60μm for both the specimen with no flaws and the one with the horizontal flaw, and 19.80μm for the specimen with the vertical flaw.

It is so clear that the horizontal flaw has practically no effect with reference to the adopted loading condition.

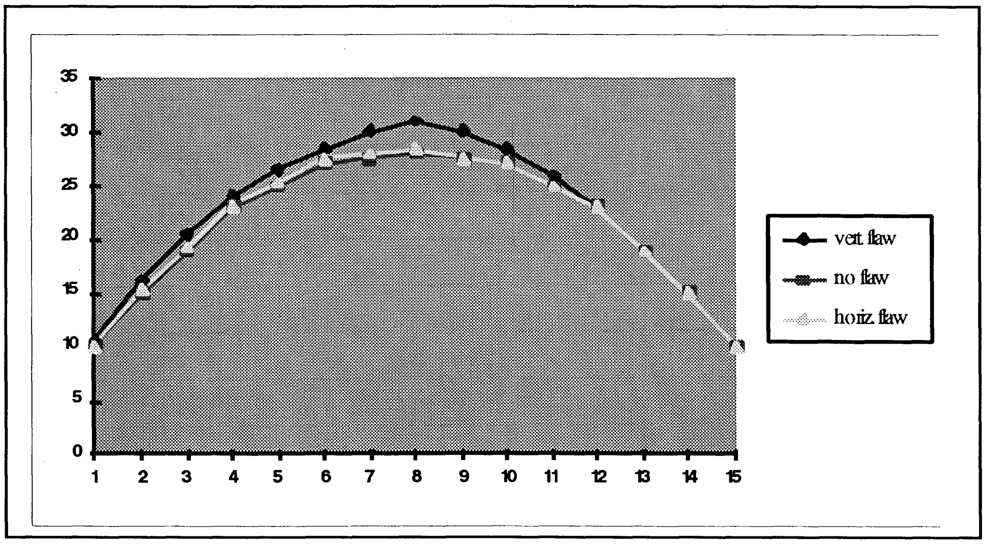

Figure 11.

5.2. Numerical Procedure. The numerical processing of the boundary experimental data was based on the above proposed gap functional (36).

Somigliana's identity (34) has been written for the problem at hand making reference to the fundamental solution for plane stresses and to the elastic state of the tested specimen.

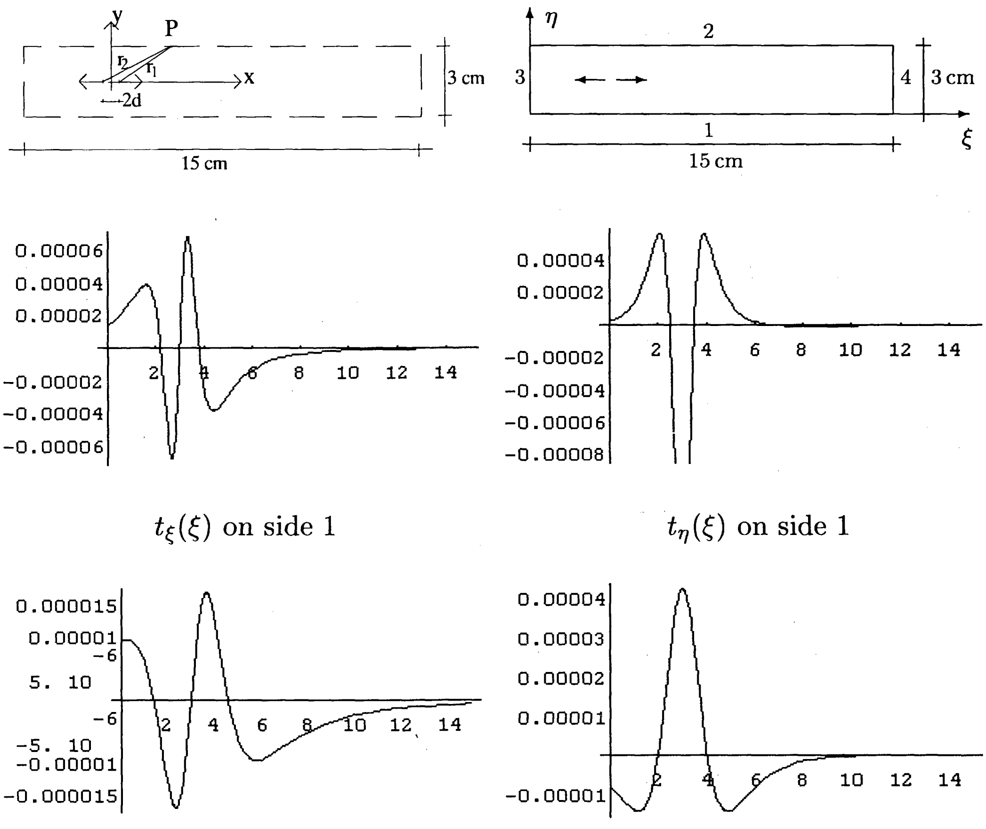

$t_\xi(\xi)$ on side 1 $t_\eta(\xi)$ on side 1

$t_\xi(\xi)$ on side 2 $t_\eta(\xi)$ on side 2

Figure 12-a.

Displacement and traction fields of the Kelvin's dipole solution for the region under analysis are

$$
\begin{aligned}
u_i^*(\mathbf{x}) &= -\frac{1}{8\pi(1-\nu)\mu}\left[(3-4\nu)\ln(r_1)\,\delta_{i1} - r_{1,i}\,r_{1,1}\right] \\
&\quad +\frac{1}{8\pi(1-\nu)\mu}\left[(3-4\nu)\ln(r_2)\,\delta_{i1} - r_{2,i}\,r_{2,1}\right],
\end{aligned}
$$

$$
\begin{aligned}
t_i^*(\mathbf{x}) \;=\; & -\frac{1}{4\pi(1-\nu)\,r_1} \\
& \cdot\left\{[(1-2\nu)\,\delta_{i1} + 2\,r_{1,i}\,r_{1,1}]\,\frac{\partial r_1}{\partial n} - (1-2\nu)\,(r_{1,i}\,n_1 - \,r_{1,1}\,n_i)\right\} \\
& + \frac{1}{4\pi(1-\nu)\,r_2} \\
& \cdot\left\{[(1-2\nu)\,\delta_{i1} + 2\,r_{2,i}\,r_{2,1}]\,\frac{\partial r_2}{\partial n} - (1-2\nu)\,(r_{2,i}\,n_1 - \,r_{2,1}\,n_i)\right\}
\end{aligned}
$$

where, with the symbols represented in fig. 12.a, we have

$$
\mathbf{x} = (x, y)\ ,\quad \mathbf{r}_1 = (x-d, y)\ ,\quad \mathbf{r}_2 = (x+d, y)\ ,
$$

$$
r_1 = (\mathbf{r}_1 \cdot \mathbf{r}_1)^{\frac{1}{2}}\ ,\quad r_2 = (\mathbf{r}_2 \cdot \mathbf{r}_2)^{\frac{1}{2}}\ .
$$

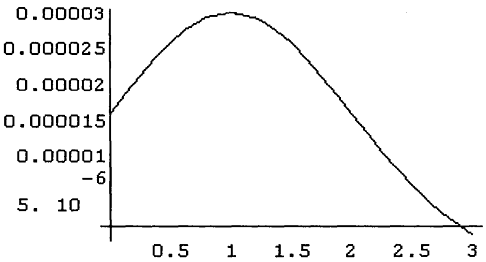

$t_\xi(\eta)$ on side 3

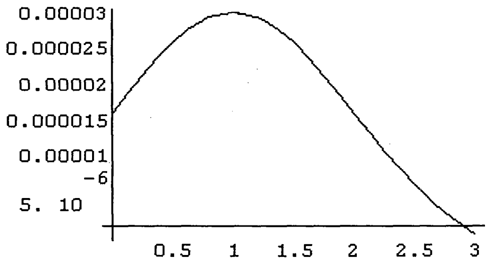

$t_\eta(\eta)$ on side 3

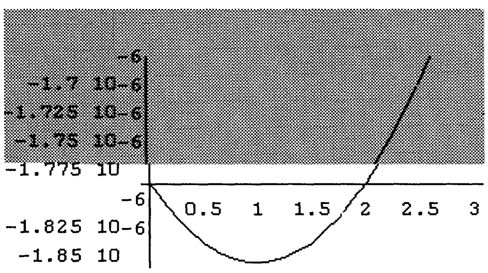

$t_\xi(\eta)$ on side 4

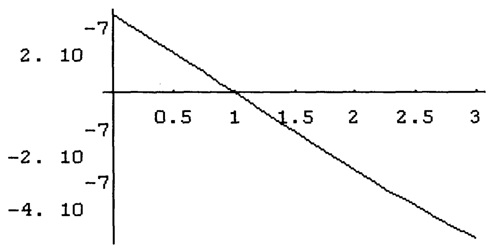

$t_\eta(\eta)$ on side 4

Figure 12-b.

Figg. 12.a and 12.b represent the traction fields of the Kelvin's dipole fundamental solution with reference to the four sides of the specimen.

The above defined gap functional G, i.e.,

$$G = -\int_{\partial\Omega_t} \mathbf{t}^* \mathbf{v}\; dS + \int_{\partial\Omega_u} \delta\mathbf{r}\; \mathbf{u}^* dS$$

in the present statically determined case, can be simplified as it results $\delta\mathbf{r} = \mathbf{0}$. Therefore we have

$$G = -\int_{\partial\Omega_t} \mathbf{t}^* \mathbf{v}\; dS \tag{38}$$

and this term can be evaluated by means of the sole boundary data.

Values of the gap function have been obtained for a mesh of internal points of the specimen with the vertical flaw. The boundary displacement field was given by the difference $\mathbf{v} = \overline{\mathbf{u}} - \mathbf{u}$ between the experimentally mapped displacement field of the specimen without flaws and the one of the specimen with the vertical flaw.

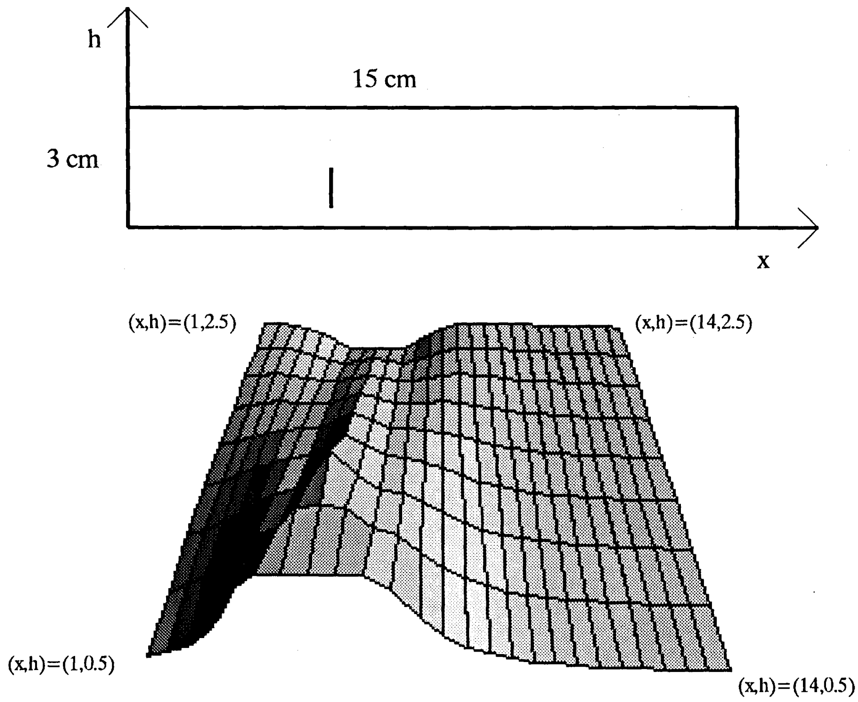

Figure 13.

In fig. 13 a plot of the function G as a function of the difference field $\mathbf{v}$ is represented. The highest values of the function G identify the position and the shape of the inner fracture and validate the proposed boundary integral approach.

6. Mathematical Considerations

At the end of our discourse the following question naturally arises: must the comparison between the boundary data necessary for the identification procedure regard the whole boundary of the bodies or is it possible to limit the analysis to a suitable sub-region of the boundary itself?

On account of the local uniqueness property of the elastic equilibrium problems we can affirm that the analysis might be indeed limited to a suitable sub-region of the boundary. In fact the solutions of the problem of elastic equilibrium for the same solid subject to distinct load and constraint conditions always differ on every sub-domain of the volume or the boundary.

This local uniqueness property can be stated by means of the following theorem [Markusevic, 1988; Michajlov, 1984; Smirnov, 1982]:

Kovalewskaja's theorem. *If the data of the problem (1.1), (1.2) and (1.3) are all analytical and the boundary surface of V is regular and simply connected in E^3, then a neighbourhood I_x of any point $\mathbf{x} \in \partial V$ will exist such that in $I_x \cap \partial V$ the elastic equilibrium problem admits a unique analytical solution.*

From the previous theorem it derives that a sub-domain V_1 of V which contains the boundary surface and presents an unique analytical solution always exists. Moreover for the analytical functions the following fundamental property holds true: *if two analytic functions coincide in a sub-domain V_1 of V, they coincide in V.* The local uniqueness of the elastic equilibrium problem follows straightforwardly.

The following theorem [Almansi, 1907] supports and widen the previous results:

Almansi's theorem. *Let an elastic body V with null volume forces be loaded on the sole free boundary ∂V_t; if the displacement and the tractions are zero for all the points of a region ∂V_o of the free boundary, then the displacements, the deformations and the stresses result identically zero in V as well.*

This theorem naturally embeds the local uniqueness principle: if two displacement fields coincide on any region ∂V_o of the loaded boundary and the tractions do the same as well, then the displacement fields coincide all over the body.

It seems so possible to limit our attention to particular boundary subsets, which we call "identification windows". It seems also obvious that these "windows" must be carefully chosen, so that the gap functional can give useful information, but these considerations exceed the limits of the present study.

References

[1] ALMANSI, E., Un teorema sulle deformazioni elastiche dei solidi isotropi, *Rendic. R. Accad. dei Lincei*, ser. 5, **XVI** (1907).

[2] BITTANTI, S., MAIER, G., NAPPI, A., Inverse problems in structural elasto-plasticity, a kalman filter approach, in "Plasticity Today" (A. Sawczuk and G. Bianchi, Eds.), Elsevier, 1984, 311–321.

[3] BUI, H.D., "Introdution aux Problemes Inverses en Mecanique des Materiaux", Eyrolles, Paris, 1993.

[4] BUI, H.D., TANAKA, M. (EDS.), "Inverse problems in engineering mechanics", A.A Balkema, Rotterdam, 1994.

[5] GUARRACINO, F., MALLARDO, V., MINUTOLO, V., NUNZIANTE, L., On a boundary integral appoach for the identification of structural defects: theory and experiments, in "Proceedings of the International Workshop on Structural Damage Assessment using Advanced Signal Processing Procedures", Pescara, Italy, 1995.

[6] LIPPMANN, H., "Engineering Plasticity - Theory of Metal Forming Processes", Springer, Berlin, 1977.

[7] MARKUSEVIC, A.I., "Elementi di Teoria delle Funzioni Analitiche", Editori Riuniti, Mir, Moscow, 1988.

[8] MICHAJLOV, V.P., "Equazioni Differenziali alle Derivate Parziali", Editori Riuniti, Mir, Moscow, 1984.

[9] MROZ, Z., Variational methods in sensitivity analysis and optimal design, *European Journal of Mechanics* **13** (1994), 115–147.

[10] MURA, T., "Micromechanics of Defects in Solids", Northwestern University, Evanston, Illinois, 1982.

[11] NATKE, H.G., The progress of engineering in the field of inverse problems: system identification, in "Inverse Problems in Engineering Mechanics" (H.D. Bui and M. Tanaka, Eds.), A.A. Balkema, Rotterdam, 1994.

[12] NUNZIANTE, L. ET AL., Theoretical tools in structural identification problem, in "Proceedings XII Congresso Nazionale AIMETA", Napoli, Italy, 1995.

[13] POPELAR, C.H., KANNINEN, M.F., "Advanced Fracture Mechanics", Oxford Univ. Press, New York, 1985.

[14] RICE, J.R., Mathematical analysis in the mechanics of fracture, in "Fracture" (H. Liebowitz, Ed.), Acad. Press, 1968.

[15] SANTANA, F., VOGELIUS, M., A computational algorithm to determine cracks from electrostatic boundary measurements, *Int. J. Eng. Sci.* **29** (80) (1991), 917–937.

[16] SMIRNOV, V.I., "Corso di Matematica Superiore", vol IV, Second Part, Editori Riuniti, Mir, Moscow, 1988.

[17] TICHONOV, A., ARSENIN, V., "Solutions of Ill-Posed Problems", Winston & Sons, Washington, 1977.

[18] VILLAGGIO, P., "Qualitative Methods in Elasticity", Noordhoff International Publishing, Leyden, 1977.